High-Resolution Measurement and Spectral Overlap of Cross-Phase Modulation Induced Spectral Broadening

Keang-Po Ho, *Member, IEEE*, Haitao Yu, Lian-Kuan Chen, and Frank Tong, *Senior Member, IEEE*

***Abstract*—Cross-phase modulation induced spectral broadening in WDM systems is measured using a high-resolution optical spectrum analyzer. The measured spectra are consistent with recently developed theoretical models. Using the theoretical models, the spectral overlap between two adjacent WDM channels is estimated for a typical 10-Gb/s system having 50 GHz of channel spacing. For -20 dB overlap, the product of number of fiber spans and optical power per channel must be less than 18.1 and 15.5 dBm for standard and nonzero-dispersion-shifted fiber, respectively.**

***Index Terms*—Cross-phase modulation, spectral broadening, WDM systems.**

I. Introduction

Optical networks using wavelength-division-multiplexing (WDM) techniques are revolutionizing broad-band networks by providing enormous communication bandwidth up to several terabits per second per fiber. However, nonlinear effects such as self-phase modulation (SPM), four-wave mixing (FWM), and cross-phase modulation (XPM) [1]–[2] affect the system when multiple channels are transmitted through the same fiber. XPM is an effect in which the optical phase of each channel is modulated by the overall optical power in the fiber because of the power-dependence of refractive index. Consequently, the optical spectrum of each WDM channel is broadened [2]–[6], limiting the transmission distance of optical signal in dispersive fiber by either phase noise to intensity noise conversion [7]–[10] or spectral overlap [3]–[5].

As summarized in [2], most previous studies of XPM-induced spectral broadening focused on single or periodic pulse interaction, but the WDM system transmits a random data stream. The measurement of [3] showed that the transmission distance of a WDM system might be limited by spectrum overlap of two WDM channels after many fiber spans. The root-mean-squared (rms) bandwidth of XPM induced spectral broadening is theoretically derived and experimentally measured in [4]. The power spectral density is theoretically derived in [5] and has significant difference with the linearized model of [6] at high power.

In this letter, we will first verify the accuracy of the exact power spectral density in [5] through high-resolution measurement of XPM induced spectral broadening. The models of [4] and [5] for XPM and [11] and [12] for SPM are then used together to predict the spectral overlap between two WDM channels.

Manuscript received March 27, 2000; revised June 6, 2000. This work was supported in part by an Earmarked Grant from the Research Grant Council of HKSAR under project CUHK 4225/00E.

K.-P. Ho is with the Department of Information Engineering, The Chinese University of Hong Kong, Shatin, NT, Hong Kong and with StrataLight Communications, San Jose, CA 95192 USA (e-mail: kpho@ie.cuhk.edu.hk)

H. Yu, L.-K. Chen, and F. Tong are with the Department of Information Engineering, The Chinese University of Hong Kong, Shatin, NT, Hong Kong.

Publisher Item Identifier S 1041-1135(00)09598-7.

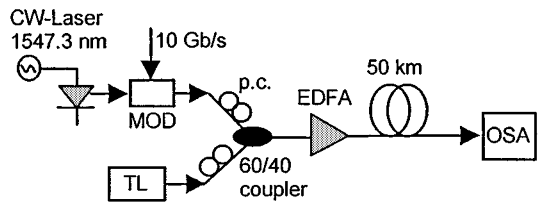

Fig. 1. Experimental setup to measure XPM induced spectral broadening.

II. High-Resolution Spectrum Measurements

The experimental setup in Fig. 1 is used to measure XPM induced spectral broadening and compared with the theory in [5]. The pump and probe setup of Fig. 1 is the same as the setup of most other experimental or theoretical studies [4]–[10]. A continuous-wave laser at a wavelength of 1547.3 nm is externally modulated using 10-Gb/s $2^{31} - 1$ pseudorandom binary sequence (PRBS) as the pump signal. The laser is dithered by a low-frequency sinusoidal wave to suppress stimulated Brillouin scattering (SBS). The probe signal is a tunable laser (TL) having longer wavelength. The pump and probe signal are combined using a coupler and amplified together using a high-power erbium-doped fiber amplifier (EDFA) having a total output power of 20.3 dBm. The probe is about 18 dB weaker than the pump signal. A high-resolution optical spectrum analyzer (OSA), known as Walics from Photonetics, is used after $L = 50$ km of standard single-mode fiber to measure spectral broadening. The OSA has a full-width at half-maximum (FWHM) resolution bandwidth of 0.018 nm, corresponding to a frequency resolution of 2.25 GHz.

Fig. 2 shows the theoretical, modified-theoretical, and measured spectra of the setup of Fig. 1. The fiber nonlinear coefficient is $\gamma = 2.27$/km/W, measured in [4], fiber loss coefficient is $\alpha = 0.20$ dB/km, and the fiber dispersion coefficient is $D = 17$ ps/km/nm. The theoretical model assumes a super-Gaussian pulse shape of $p(t) = P_0 \exp[-(t/T_0)^4]$ with

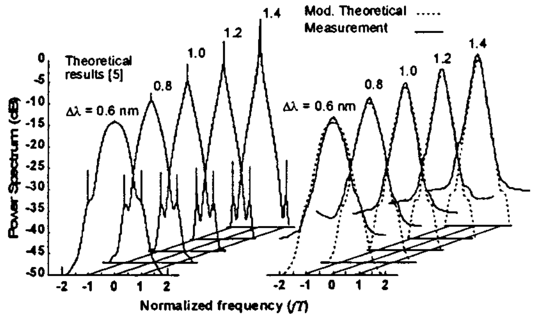

Fig. 2. Theoretical, modified-theoretical, and measured power spectrum of XPM induced spectral broadening.

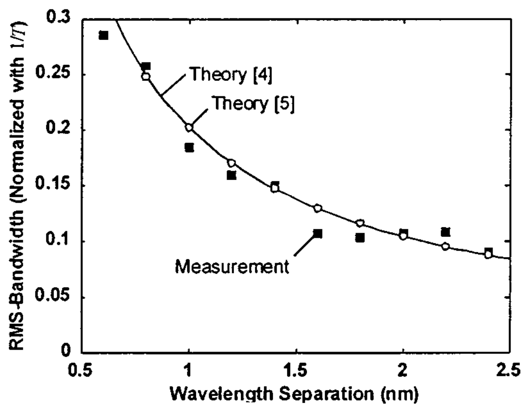

Fig. 3. RMS-bandwidth versus wavelength separation.

1/e-width of $T_0 = 0.55T$, corresponding to a FWHM pulse width of T, where P_0 is the peak power, and $T = 100$ ps is the bit interval for 10-Gb/s system. The theoretical results are that of [5] with a resolution bandwidth of 39 MHz, i.e., 10 000/256 MHz, where 256 provides simple calculation procedure. Because the theoretical results cannot compare with the measured results due to the difference in resolution bandwidth, the modified theoretical results are that of [5] with a resolution bandwidth of 2.25 GHz, corresponding to that of the OSA. The discrete lines in the theoretical results correspond to the delta-function in [5]. The flat tail of the measured results is due to the amplified spontaneous noise (ASE) from the EDFA. Fig. 2 shows that the exact spectrum of [5] is consistent with the high-resolution measurement by comparing the modified-theoretical results with actual measurements.

Fig. 3 shows the rms-bandwidth of spectral broadening calculated from the spectra of Fig. 2. The measured rms-bandwidth is calculated by just taking the part of spectrum larger than −30 dB from the peak (to eliminate the effects of ASE from the EDFA) and subtracting the effects of OSA resolution filter. Fig. 3 also shows that the measured rms-bandwidth is consistent with the models of [4] and [5].

A launched power of 20.3 dBm per channel in Fig. 1 is not practical for real WDM system. For a M-span WDM system with prefect dispersion compensation in each fiber link, from both [4] and [5], the overall spectral broadening is approximately equal to a single-span WDM link having an optical power of MP_{av}, where P_{av} is the optical power per fiber span. Therefore, the spectra of Figs. 2 and 3 are approximately the same as that of a WDM system with 100 spans and 0.3 dBm per channel per fiber span, or other combinations having $MP_{av} = 20.3$ dBm.

Both the theories of [4] and [5] assume that optical pulse remains the same along all fiber spans. In practice, fiber dispersion distorts the optical pulse, especially for system having strong SPM/XPM [2]. However, calculation in [4] and [5] and [11] and [12], the measurements of Figs. 2 and 3, and those of [4] and [11] indicate that the assumption is valid for the studies of SPM/XPM induced spectral broadening.

III. Spectral Overlap

Figs. 2 and 3 may conclude that the theoretical models in [4] and [5] are valid. The models of [5] for XPM induced spectral broadening can be used to find the spectral overlap between two WDM channels. The power spectrum of a WDM channel is contributed by three factors:

1) original signal spectrum;
2) SPM from the channel itself;
3) XPM from all other WDM channels.

The contribution from the original signal and SPM, or simply the WDM channel itself, can be evaluated from the models of the early works of [11] and [12]. In the single-pulse analysis, for an input zero-chirp pulse of $p(t)$, the pulse spectrum at the fiber output is $|P_o(f)|^2$, where $P_o(f)$ is the Fourier transform of $\sqrt{p(t)}\, e^{-j\gamma L_e p(t) - \alpha L/2}$, with $L_e = (1 - e^{-\alpha L})/\alpha$ being the effective nonlinear fiber length. For a WDM channel with random data stream, the spectral density at the fiber output is [13]

$$S_0(f) = \frac{1}{4T}|P_o(f)|^2 + \frac{1}{4T^2} \sum_{k=-\infty}^{\infty} \left| P_o\left(\frac{k}{T}\right)\right|^2 \delta\left(f - \frac{k}{T}\right). \tag{1}$$

Because all WDM channels are independent of each other, the overall power spectral density is the convolution of the spectral densities, i.e.,

$$S_T(f) = S_0(f) \otimes S_1(f) \otimes \cdots \otimes S_K(f) \tag{2}$$

where $\otimes$ denotes convolution, and $S_k(f)$ and $k = 1, 2, \cdots, K$ are the spectral densities due to XPM induced spectral broadening from other WDM channels [5]. The spectral overlap factor is

$$xt = \frac{\displaystyle\int_{\Delta f/2}^{\infty} S_T(f)\, df + \int_{-\infty}^{-\Delta f/2} S_T(f)\, df}{\displaystyle\int_{-\infty}^{\infty} S_T(f)\, df} \tag{3}$$

where Δf is the frequency spacing between two WDM channels. The factor in (3) assumes that adjacent WDM channels have the same spectral density and the WDM filter is an ideal filter.

Fig. 4 shows the spectral overlap factor as a function of optical power MP_{av} for standard and nonzero dispersion shifted fiber (NZDSF) having a dispersion coefficient D of 17 and 4 ps/km/nm, respectively. The channel separation is $\Delta\lambda = 0.4$

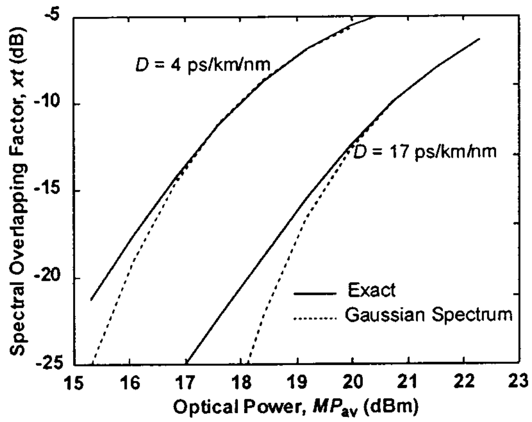

Fig. 4. Spectral overlap factor versus optical power.

nm, corresponding to a frequency separation of 50 GHz. Fig. 4 is for the central channel of an 11-channel WDM system. Because far-away channels contribute very little spectral broadening into the center channel (see Fig. 3), Fig. 4 can be used to approximate the spectral overlap of a WDM system having more than 11 channels.

From the central-limit theorem, the convolution of many *more or less the same* functions evolves to Gaussian probability density function [14]. The overall power spectral density in (2) may be approximated by a Gaussian spectrum. Fig. 4 also shows the power overlap factor calculated using the Gaussian spectrum approximation in which the overall rms-bandwidth is the root-summation-squared of those contributions from SPM [12] and XPM [4], respectively, resulting with substantially reduced computation time. The spectral overlap factor is approximated given by

$$xt \approx \mathrm{erfc}\left(\frac{\Delta f}{2\sqrt{2}\,W_{\mathrm{rms}}}\right) \quad (4)$$

where $\mathrm{erfc}(\cdot)$ is the complementary error function, and W_{rms} is the overall rms bandwidth.

From Fig. 4, the assumption of Gaussian spectrum may underestimate the spectral overlap and system performance degradation. The discrepancy between the Gaussian approximation and exact model is because the original signal contributes most to the overall spectrum at low optical power. SPM and XPM gives larger spectral broadening at high launched power, and Gaussian spectrum approximation provides the same spectral overlap factor as the exact model. The ratio of the rms-bandwidths from SPM (without counting the original signal spectrum) to XPM is 2.6 and 0.8 for standard and NZDSF fiber, respectively, independent of launched optical power.

Optical filters cannot separate two WDM channels when their spectra overlap with each other, resulting in homodyne crosstalk [15]. For a conservative estimation and certain margin for optical filtering, the spectrum overlap factor should be less than -20 dB [15]. The maximum power limits in MP_{av} are 18.1 and 15.5 dBm for standard and NZDSF fiber, respectively. The limitation in MP_{av} provides a bound in either the number of fiber spans or the launched power in each fiber span.

Although the Gaussian spectrum approximation underestimates the spectral overlap and provides larger power limits, the discrepancy between Gaussian spectrum approximation and exact model is less than 0.6 dB for spectral overlap factor larger than -20 dB. Therefore, the assumption of Gaussian spectrum may provide a rough estimation of the power limits within a short computational time. Its accuracy improves with the increase of optical power.

IV. Conclusion

A high-resolution OSA is used to measure the power spectral density of XPM induced spectral broadening. The measured spectra are consistent with recently developed theoretical models for spectral density and rms bandwidth. The spectrum of a WDM channel is evaluated by the convolution of the spectra from the original signal with SPM and XPM induced spectral broadening from all adjacent channels. For a spectral overlap factor less than -20 dB, the power limits in terms of MP_{av} are 18.1 and 15.5 dBm for standard and NZDSF fiber, respectively, limiting either the maximum number of fiber spans or the launched power per channel per span.

References

[1] A. R. Chraplyvy, "Limitation on lightwave communications imposed by optical-fiber nonlinearities," *J. Lightwave Technol.*, vol. 8, pp. 1548–1557, 1990.

[2] G. P. Agrawal, *Nonlinear Fiber Optics*, 2nd ed. San Diego, CA: Academic, 1995, pp. 278–285.

[3] V. Mikhailov, R. I. Killey, J. Prat, and P. Bayvel, "Limitation to WDM transmission distance due to cross-phase modulation induced spectral broadening in dispersion compensated standard fiber systems," *IEEE Photon. Technol. Lett.*, vol. 11, pp. 994–996, 1999.

[4] K.-P. Ho, E. Kong, L. Y. Chan, L.-K. Chen, and F. Tong, "Analysis and measurement of root-mean-squared bandwidth of cross-phase modulation induced spectral broadening," *IEEE Photon. Technol. Lett.*, vol. 11, pp. 1126–1128, 1999.

[5] K.-P. Ho, "Spectral density of cross-phase modulation induced phase noise," *Opt. Commun.*, vol. 169, pp. 63–68, 1999.

[6] T. K. Chiang, N. Kagi, M. E. Marhic, and L. G. Kazovsky, "Cross-phase modulation in fiber links with multiple optical amplifiers and dispersion compensators," *J. Lightwave Technol.*, vol. 14, pp. 249–259, 1996.

[7] L. Rapp, "Experimental investigation of signal distortions induced by cross-phase modulation combined with dispersion," *IEEE Photon. Technol. Lett.*, vol. 9, pp. 1592–1594, 1997.

[8] R. Hui, Y. Wang, K. Demarest, and C. Allen, "Frequency response of cross-phase modulation in multispan WDM optical fiber systems," *IEEE Photon. Technol. Lett.*, vol. 9, pp. 1271–1273, 1998.

[9] G. Bellotti, M. Varani, C. Francia, and A. Bononi, "Intensity distortion induced by cross-phase modulation and chromatic dispersion in optical-fiber transmission with dispersion compensation," *IEEE Photon. Technol. Lett.*, vol. 10, pp. 1745–1747, 1998.

[10] A. V. T. Cartaxo, "Cross-phase modulation in intensity modulation-direct detection WDM systems with multiple optical amplifiers and dispersion compensators," *J. Lightwave Technol.*, vol. 17, pp. 178–190, 1999.

[11] R. H. Stolen and C. Lin, "Self-phase modulation in silica optical fibers," *Phy. Rev. A*, vol. 17, pp. 1448–1453, 1978.

[12] S. C. Pinault and M. J. Potasek, "Frequency broadening by self-phase modulation in optical fibers," *J. Opt. Soc. Amer. B.*, vol. 2, pp. 1318–1319, 1985.

[13] J. G. Proakis and M. Salehi, *Communication Systems Engineering*. Englewood Cliffs, NJ: Prentice-Hall, 1994, pp. 537–541.

[14] W. B. Davenport Jr. and W. Root, *An Introduction to the Theory of Random Signals and Noise*. New York: IEEE , 1987, pp. 81–84.

[15] K.-P. Ho, "Analysis of homodyne crosstalks in optical networks using Gram–Charlier series," *J. Lightwave Technol.*, vol. 17, pp. 149–154, 1999.